Study and simulation of electron transport in Ga$_{0.5}$In$_{0.5}$Sb based on Monte Carlo method

© A.A. El Ouchdi [1,2], B. Bouazza [1], Y. Belhadji [1,3], N. Massoum [1]

[1] Research Unit of Materials and Renewable Energies, Abou Bakr Belkaid University,
Tlemcen, Algeria
[2] Centre de Développement des Technologies Avancées,
Algiers, Algeria, Division of Microelectronics & Nanotechnologies
[3] Electrical and engineering department, Faculty of applied sciences, University of Tiaret,
Tiaret, Algeria

E-mail: elouchdi.amine@gmail.com

This work addresses the issue related to the electronic transport in the III−V ternary material Ga$_{0.5}$In$_{0.5}$Sb using Monte Carlo method. We investigated the electronic motion in the three valleys Γ, *L*, and *X* of the conduction band. These three valleys are isotropic, non-parabolic and centred on the first Brillouin zone. In our study, we included scatterings with ionised impurities, acoustic and polar optical phonons, as well as, intervalley and intravalley interactions. We discussed the electronic transport characteristics at the stationary and the transient regimes in function of temperature and electric field.

1. Introduction

The need of electronic devices operating under strength constraint environments, such as high electric field, high temperature and high frequency, has pushed the research toward the fabrication of electronic devices based on ternary and quaternary materials with two variants, namely, III−V or II−VI groups [1]. Indeed, the narrow bandgap antimonide based compound semiconductors are regarded as good materials operating on such circumstances. Among antimonies, the gallium indium antimonide (Ga$_x$In$_{1-x}$Sb) owning a stoichiometric coefficient *x* crystallising and following zinc-blende structure have gain high attention of researchers. The first interests granted to the Ga$_x$In$_{1-x}$Sb goes back to the seventies of the last century, where its fundamental properties were introduced [2,3]. Through time, investigations continued to growth up significantly going from simple GaInSb structures to more complexes heterostructure based electronic devices such as, laser diodes and transistors, etc. [4–9]. In fact, the features of this material include those of GaSb and InSb materials such as low direct band-gap (from 0.17 to 0.72 eV), high mobility (from 5000 to 80 000 cm^2/Vs) and low effective masses (from 0.014 m_e to 0.042 m_e) [10]. Moreover, Ga$_x$In$_{1-x}$Sb properties can be adjusted following Vegard's laws only by controlling the stoichiometric coefficient *x*.

GaInSb is an important material for the microelectronics, since it is used for the fabrication of the third generation of high-electron mobility transistors (HEMT), heterojunction bipolar transistor (HBT) devices, as well as, ultra-high speed, ultra-lower power consumption and good noise performance integrated circuits [11]. Furthermore, antimonies based materials are the most suitable for the design of third-generation Infrared detectors [11]. Also, in infrared lasers, it can be used in chemical detection, biomedical diagnostics, satellite remote sensing technology and thermo-photovoltaics cells [12].

This paper goes through three main steps; the first part gives an overview of the Monte Carlo method, the second part show results of different interactions in function of the energy, while the final part aims at highlighting the drift velocity in both stationary and transient regimes.

2. Description of the method

The Monte Carlo method gives a precise solution of studying the non-equilibrium carrier transport in semiconductor based electronic devices at high electric field and high temperature. This method is used for the resolution of Boltzmann equation which considers the distribution function variation of electrons in movement.

In this method, the dynamics of electrons passes through two steps, free flights and scatterings with the network. During the free flight, the evolution of position and wave vector as function of time in the absence of the external field is given by the following equations:

$$\begin{cases} \dfrac{dk}{dt} = \dfrac{1}{\hbar} eE, \\[2mm] \dfrac{dr}{dt} = \dfrac{\hbar}{m^*} k. \end{cases} \quad (1)$$

Where *E* represents the electric field, *k* stands for the electron wave vector, *r* refers to the position vector and *e* is the electron charge.

Time of flight is calculated by self scattering approach which aims to introduce an additional interaction. This interaction does not affect the electron motion and makes the total interaction probability Γ constant. Time of flight

can be calculated using a random number r which varies between 0 and 1 as expressed in Eq. (2):

$$\Delta t = -\frac{1}{\Gamma} \ln(r). \qquad (2)$$

Under an electric field, electrons change from their initial state (r_i, k_i) at time t_i to the final state (r_f, k_f) at time t_f, during a short time δt. Therefore, the electron movement in absence of interactions can be described by the following equations [13]:

$$\begin{cases} k_f = k_i - \dfrac{\delta t}{\hbar}\, eE, \\[2mm] r_f = r_i - \dfrac{\hbar}{m^*}\, \dfrac{(k_i + k_f)}{2}\, \delta t. \end{cases} \qquad (3)$$

Besides the time of flight, scattering mechanisms are also selected stochastically using probabilities related to the microscopic behaviour description. If the interaction is fictive, the state of the electron is kept unchanged. However, after interaction, the new position and the wave vector are redefined.

3. Simulation results

The simulation is carried out using the Ensemble Monte Carlo simulator described in FORTRAN language. This simulator identifies the electron motion in the three valleys of the conduction band Γ, L, and X which are isotropic and non-parabolic [14]. The definition of the band structure is an inescapable step to perform the simulation, because it enables to introduce the required parameters, such as, bandgap, effective masses, non-parabolic coefficients, etc. In order to approach the actual conditions, the simulator takes in account scatterings with ionised impurities, acoustic and polar optical phonons, as well as, intervalley and intravalley interactions.

3.1. Electronic interactions

A. Ionised impurities interactions

Fig. 1 sketches the evolution of ionised impurities interactions as function of energy for each valley. These interactions are described through the screened Coulomb potential of the Brooks Herring [15]. As seen, the values of these interactions are high at low energy, whereas they get weak sharply when energy increases.

B. Acoustic interactions

Fig. 2 depicts the evolution of acoustic interactions as function of the energy for each valley. The acoustic interactions are neglected for Γ valley while they increase monotonically with energy for the valleys L and X. These interactions are elastics with insignificant influence on the electrons since their final energy remains constant.
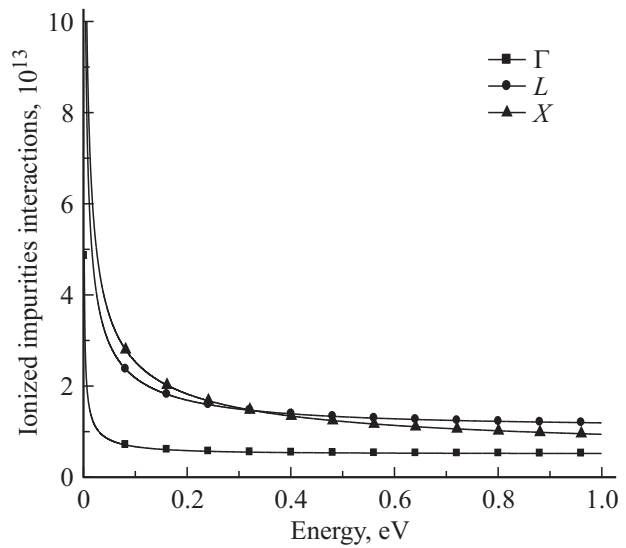
Figure 1. Ionized impurities interactions.
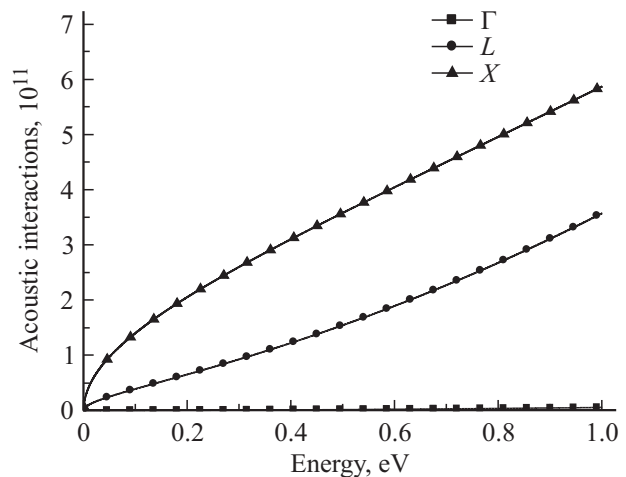
Figure 2. Acoustic interactions.

C. Polar optical interactions

The evolution of polar optical interactions versus energy for the mentioned valleys in the case of emission and absorption is represented in Fig. 3. These interactions are important in all valleys and they own the ability of absorption or emission of optical phonons. The emission of phonons occurs only when electrons energy is higher than the polar optical phonon, namely, 27 meV. Note that, emission interactions are more important than those of absorptions.

D. Intervalley interactions

The possible transitions between the three valleys Γ, L and X in case of absorption and emission are shown in Fig. 4. These transitions are accomplished by absorbing or emitting phonons which depends on the difference of energy
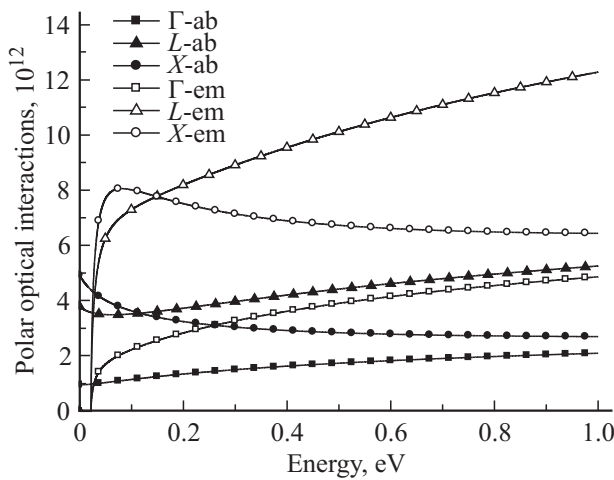
Figure 3. Polar optical interactions.
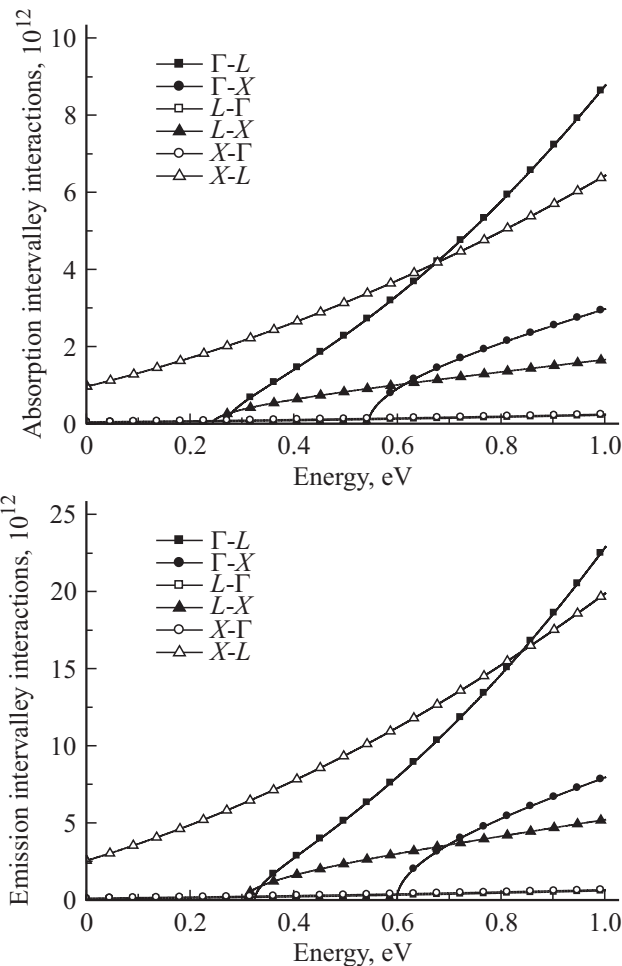
Figure 4. Absorption and emission intervalley interactions.

between outgoing and incoming valleys. The transition to upper valleys occurs only when carrier's energy is higher than the separation energy between different valleys, i.e. 0.297 for $\Delta E \Gamma L$, 0.57 for $\Delta E \Gamma X$ and 0.28 for $\Delta E L X$.

E. Intravalley interactions

Fig. 5 illustrates the evolution of L and X intravalley interactions versus energy for both emission and absorption. These transitions occur between equivalent valleys existing only in L and X. From the figure, it can be concluded that these interactions increase with the carrier's energy, and reach higher values for X valley.

3.2. Electron drift velocity

A. Effect of temperature of the drift velocity in stationary regime

The electronic drift velocity as function of the electric field at different values of temperature is represented in Fig. 6. As see, for low values of electric field, the mentioned characteristics are linear; in this case, electrons are situated in Γ valley where they have high mobility and low effective mass. The predominant acoustic phonon scatterings is the main factor behind the occurrence of such linear behaviour. The electronic drift velocity showed
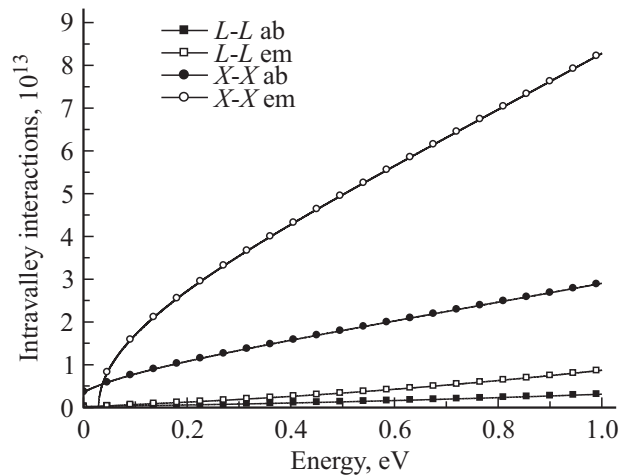
Figure 5. Intravalley interactions.
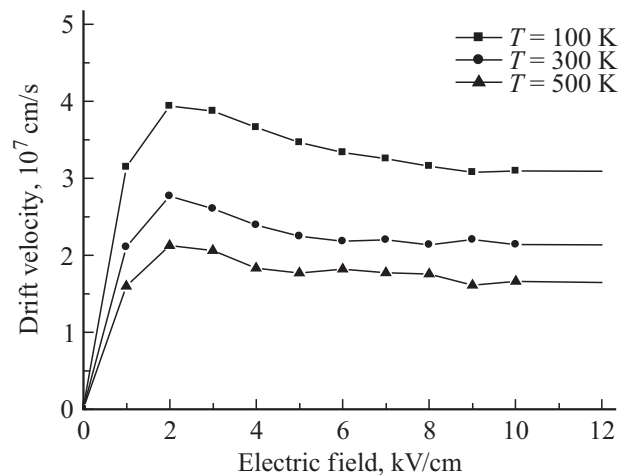
Figure 6. Drift velocity vs electric field at different temperature.

peaks at electric field of 2 kV/cm when $T = 300$ K. At this condition, electrons are still located in Γ valley but the main interactions are performed with optical phonons. Thereafter, by increasing the electric field to high values, electrons acquired sufficient energy enabling them to move to satellite valleys, thus, the velocity decreases until establishing the stationary regime, therefore the electronic drift velocity remains constant. As we can see in the same figure, when the temperature increases the peak velocity diminishes due to the augmentation of the global scattering.

B. Effect of the temperature and the electric field of the drift velocity in transient regime

The evolution of electronic drift velocity at different values of temperature and electric field as function of time is plotted in Fig. 7. The velocity shows sharp increasing and reaches an over-speed regime typically $8 \cdot 10^8$ cm/s at temperature of 300 K, noting that, this value is higher than the stationary speed measured as $2.1 \cdot 10^7$ cm/s at the same value of temperature. This over-speed is due to the strong acceleration of electrons by the electric field, whereas, some

interactions occurred. Then, the velocity decreases until it reaches the stationary regime. In addition, high temperature leads to a decrease of the velocity peak. Furthermore, the augmentation of the electric field at a fixed value of temperature, caused precocious over-speed occurrence with more significant value, however, in such context the steady regime velocity become lower compared with weaker electric field.

4. Conclusion

In this work, the electronic transport in $Ga_{0.5}In_{0.5}Sb$ material has been investigated and carried out using the ensemble Monte Carlo simulation. The results show that acoustics and polar optics interactions were dominant at weak electric field. Consequently, the drift velocity increased linearly and achieved maximum value of $2.7 \cdot 10^7$ cm/s. However, intervalley interactions dominated at higher electric field values, with a drift velocity of $2 \cdot 10^7$ cm/s.

References

[1] S. Adachi. Proporties of Semiconductor Alloys: Group-IV, III−V and II−VI Semiconductors (Wiley, Singapore, 2009) v. 2.

[2] M. Kawashima, K. Ohta, S. Kataoka. Intern. Electron Dev. Meeting, **23**, 372 (1977).

[3] T. Ikoma, K. Sakai, Y. Adachi, H. Yanai. Electron. Lett., **10** (19), 402 (1974).

[4] A. Mitric, T. Duffar, C. Diaz-Guerra, V. Corregidor, L.C. Alves, C. Garnier, G. Vian. J. Cryst. Growth, **287** (2), 229 (2006).

[5] G. Kipshidze, T. Hosoda, W.L. Sarney, L. Shterengas, G. Belenky. IEEE Phot. Techn. Lett., **23** (5), 317 (2011).

[6] S.G. Ghalamestani, M. Ek, B. Ganjipoour, C. Thelander, J. Johansson, P. Caroff, K.A. Dick. Nano Lett., **12** (9), 4914 (2012).

[7] T. Hosoda, D. Wang, G. Kipshidze, W.L. Sarney, L. Shterengas, G. Belenky. Semicond. Sci. Techn., **27** (5) (2012).

[8] Z. Yuan. *Antimonide-based iii-v CMOS technology* (Ph.D. Thesis, Stanford University, 2013).

[9] L. Ma, W. Hu, Q. Zhang, P. Ren, X. Zhuang, H. Zhou, J. Xu et al. Nano Lett., **14** (2), 694 (2014).

[10] M. Levinshtein, S. Rumyansev, M. Shur. *Handbook series on Semiconductor Parameters: Ternary and Quaternary III−V Compounds* (World Scientific, Singapore, 1996) v. 2.

[11] C. Liu, Y. Li, Y. Zeng. Engineering, **2** (8), 617 (2010).

[12] M.G. Mauk, V.M. Andreev. Semicond. Sci. Techn., **18** (5), 191 (2003).

[13] B. Bouazza, A. Guen-Bouazza, C. Sayah, N.E. Chabanesari. J. Modern Phys., **4** (4), 121 (2013).

[14] D. Vasileska, S.M. Goodnick, G. Klimeck. *Computational Electronics: Semiclassical and Quantum Device Modeling and Simulation* (Taylor and Francis Group, Boca Raton, 2010).

[15] C. Jacoboni, P. Lugli. *The Monte Carlo Method for Semiconductor Device Simulation* (Springer, Vienna, 1989).
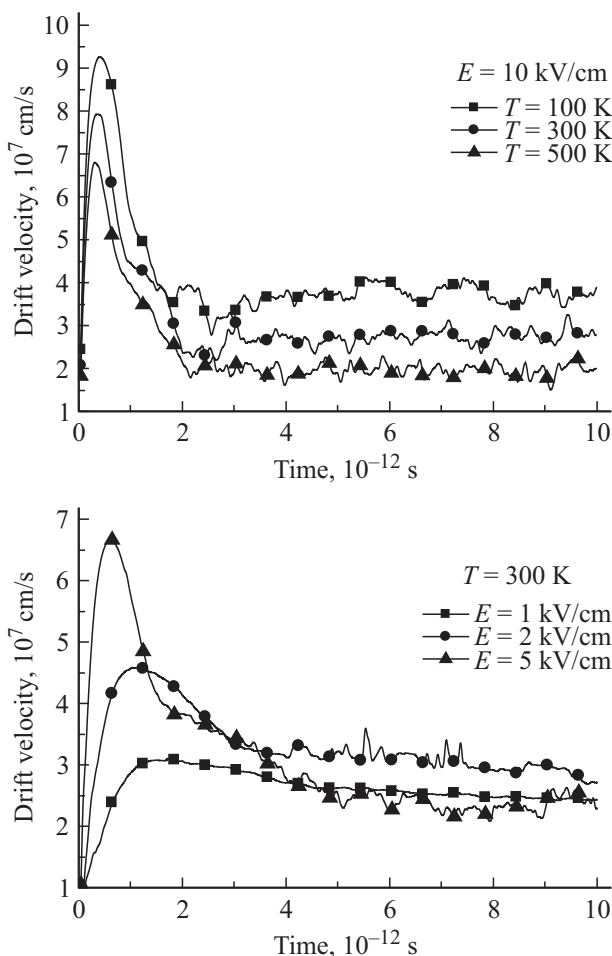
Figure 7. Drift velocity *vs* time at different electric fields and temperatures.